Chemical Science

Cite this: *Chem. Sci.*, 2012, **3**, 3315

www.rsc.org/chemicalscience

EDGE ARTICLE

Rational design of ZnSalen as a single and two photon activatable fluorophore in living cells†

Jing Jing,‡[a] Juan-Juan Chen,‡[a] Yang Hai,[a] Jinhui Zhan,[a] Pingyong Xu*[b] and Jun-Long Zhang*[a]

Received 15th June 2012, Accepted 23rd August 2012
DOI: 10.1039/c2sc20764h

Rational design of effective photoactivatable/photoswitchable fluorophores, by introducing appropriate photoreactions to tune the electron transfer processes of the ground or/and excited states and switch fluorescence off/on, is crucial to achieve high temporal and spatial resolution in live cell (organism) imaging. Besides one photon activatable fluorophores, it is highly desirable to develop two photon activatable fluorophores using light in the NIR or IR region, which reduces photodamage and allows deep penetration into cells or tissues. In this work, we describe the design of one and two photon activatable ZnSalen by incorporating thioether moieties in the 3,3′-positions which quenches the fluorescence as a result of a PET process. Through one or two photon irradiation, the thioethers can be oxidized to sulfoxides and the fluorescence of ZnSalen "switched on", due to the electron-withdrawing sulfoxides, which perturbs the PET process. We further demonstrate the application of this ZnSalen as a photoactivatable fluorophore in living cells using one and two photon fluorescence microscopies. In two photon microscopy, a high signal to noise contrast was achieved by irradiation with an 840 nm laser. Moreover, this photoactivatable ZnSalen was successfully applied in bioimaging in a model living organism *Caenorhabditis elegans* (*C. elegans*), and *ca.* 5 times fluorescence intensity increase was observed after one and two photon irradiation. This paradigm by modulation of the PET process in ZnSalen provides a promising methodology for the design of photoactivatable fluorophores in further applications in super resolution molecular imaging.

Introduction

Photoactivatable/photoswitchable fluorophores are attracting increasing attention in optical materials[1–3] and molecular imaging.[4–7] Especially since advances in single-molecule-based super-resolution techniques have broken the diffraction barrier,[8–11] it has become highly desirable to develop new photoactivatable/photoswitchable fluorophores with enhanced signal to noise ratios and large numbers of emitted photons N, because the achievable resolution scales as $1/\sqrt{N}$.[12] An impetus to develop synthetic fluorophores is provided by their advantages, such as more emitted photons, smaller size and synthetic design flexibility, over the widely used fluorescent proteins.[8,9,13,14] Therefore, the rational design of effective photoactivatable/photoswitchable fluorophores is of importance to achieve high spatial resolution. The essence of such molecular design is tuning the electron transfer processes of the ground or excited states to switch fluorescence off/on, as a result of appropriate photoreactions such as photolysis of an azide[15] or spiro-diazoketone,[16] photoisomerization of a spiropyran-merocyanine,[17] photoclick tetrazole–alkene cycloaddition,[18] and "photouncaging" of *ortho*-nitrobenzyl moieties.[19] Moreover, to reduce photodamage and autofluorescence and increase deep penetration into cells or tissues, choosing appropriate fluorophores capable of two photon activation under irradiation in the NIR or IR region has become an effective approach. Toward this goal, "photouncaging" two photon sensitive protecting groups is the most used strategy, which is dependent on the uncaging action cross-section of protecting groups.[20–22] In contrast to the "photocaging" strategy, expanding the scope of photoreactions capable of being initiated by two photon excitation is an alternative to enrich the repertoire of photoactivatable fluorophores. Herein, we described the design of a one and two photon photoactivatable ZnSalen based on photosulfoxidation, and provided an *in vivo* illustration of its off/on luminescence switching in living cells as well as in a model living organism *Caenorhabditis elegans* (*C. elegans*).

[a]*Beijing National Laboratory for Molecular Sciences, State Key Laboratory of Rare Earth Materials Chemistry and Applications, College of Chemistry and Molecular Engineering, Peking University, Beijing 100871, P. R. China. E-mail: zhangjunlong@pku.edu.cn; Fax: +86-10-62767034*
[b]*National Laboratory of Biomacromolecules, Institute of Biophysics, Chinese Academy of Sciences, Beijing 100101, P. R. China. E-mail: pyxu@moon.ibp.ac.cn; Fax: +86-10-64888524*

† Electronic supplementary information (ESI) available: Experimental section and supplementary figures. See DOI: 10.1039/c2sc20764h

‡ These authors contributed equally.

As an important class of synthetic fluorophores, luminescent metal complexes have recently emerged as biological probes in living cell imaging for the high luminescence, photostability, large Stokes shifts and long life times.[23–27] However, few of them have been designed as photoactivatable/photoswitchable fluorophores for cell imaging,[28] which limits further applications. As our continued interest in luminescent metal probes, ZnSalen (Salen = 2,3-bis[(4-dialkylamino-2-hydroxybenzylidene)amino] but-2-enedinitrile) has been employed for its high fluorescence with nonlinear optical properties as well as its large two photon absorption cross-section.[29,30] Moreover, it consists of an electron-donor (D)/electron-acceptor (A) pair with intramolecular charge transfer (ICT),[31–33] rendering a core structure for designing photoactivatable fluorophores, according to a photo-induced electron transfer (PET) mechanism.[34,35] We envisioned that, introducing an electron rich moiety to ZnSalen might induce a PET effect from this electron donor to the first excited singlet state of the fluorophore, and consequently quench the fluorescence. Upon irradiation, an appropriate photoreaction, which converts the electron rich moiety into an electron deficient moiety and lowers the energies of the frontier molecular orbitals and prevent PET and consequently cause the fluorescence to be "switched on". With this in mind, thioether groups, as functional trigger moieties, were incorporated in the 3,3′-positions of ZnSalen to generate a photoactivatable fluorophore **J-1**. Indeed, this photoactivatable ZnSalen features a great fluorometric response for one and two photon excitation, through photooxidation of the thioether moieties,[36,37] in living cells and even a model living organism *C. elegans*.

Results and discussion

Following the synthetic route in Scheme 1, we started from 3-methoxy-*N*-methylaniline **1**, through alkylation, demethoxylation, Vilsmeier reaction and aromatic alkylthiolation, and the key intermediate **5** (1,2,3,4-tetrahydro-4-methyl-6-carboxaldehyde-7-methoxy-1,4-benzothiazine) was obtained. Condensation of **5** with 2,3-diaminomaleonitrile in the presence of $Zn(OAc)_2 \cdot 2H_2O$ afforded **J-1** in a yield of 86%. The structure of **J-1** was characterized by ^{1}H-NMR, high resolution ESI-MS and FT-IR (ESI†).

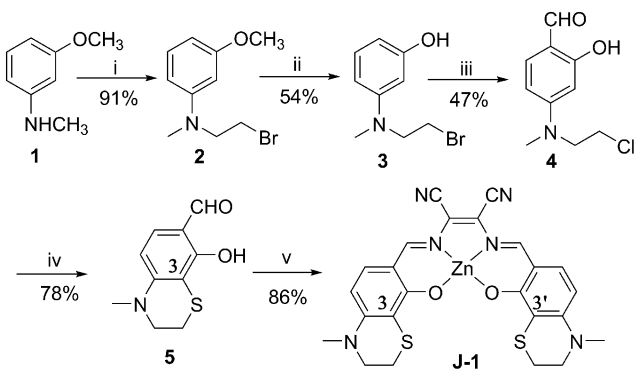

Scheme 1 Synthetic route for **J-1**: (i) $BrCH_2CH_2Br$, $KHCO_3$, CH_3CN; (ii) BBr_3, DCM, −78 °C to rt; (iii) $POCl_3$, DMF, 0 °C to rt; (iv) NaMTS, KBr, CH_3CN; (v) $Zn(OAc)_2 \cdot 2H_2O$, 2,3-diaminomaleonitrile, EtOH.

Under irradiation under a 532 nm laser (20 mW) or sunlight, a **J-1** solution in DMSO changed from non-luminescent to highly luminescent. The UV-vis spectra in Fig. 1a showed that the absorptions at 388, 437 and 597 nm blue shifted to 381, 436 and 586 nm, respectively. Interestingly, the emission dramatically increased at 623 nm (316 fold, Fig. 1b). The HR ESI-MS spectrum showed a main peak with a molecular weight of $[M + H + 32]^+$, corresponding to the addition of two oxygen atoms to **J-1**.

To identify that the product is from photosulfoxidation, we prepared **J-2** from sulfoxide **6** (Scheme 2) and characterized it using ^{1}H-NMR, HR ESI-MS and FT-IR. As depicted in Fig. 1c, the photosulfoxidation of **J-1** was monitored *in situ* by ^{1}H-NMR spectroscopy at 0, 2 and 4 h (i–iii). The resonances for the imine and phenyl moieties at δ 8.12, 7.05 and 6.33 ppm decreased and new peaks at δ 8.15, 7.39, and 7.05 ppm appeared, which were identical with those of **J-2** (Fig. 1c (iv)).

The photophysical data for **J-1** and **J-2** are summarized in Table 1. The UV-vis absorption spectrum of **J-2** displays absorptions at 381, 436 and 586 nm as depicted in Fig. S1,† corresponding to that of **J-1** after photosulfoxidation. Importantly, **J-2** is much more emissive than **J-1** with a high fluorescence quantum yield of 0.81. Upon two photon excitation by a mode-locked femtosecond Ti:sapphire laser at 840 nm, the recorded two photon induced emission spectrum of **J-2** is virtually identical to the one photon induced emission spectrum (Fig. S2†). A two photon process was confirmed by a power dependence experiment with a slope of 1.90 (Fig. S3a†). Referring to Rhodamine B, the two photon cross-section of **J-2** was estimated to be 296 GM in ethanol at 840 nm (Fig. S3b†).

We then performed time course experiments to examine several lasers with different wavelengths (488, 532 and 633 nm, 5 mW) for photoactivation of **J-1**. The yields of **J-2** were

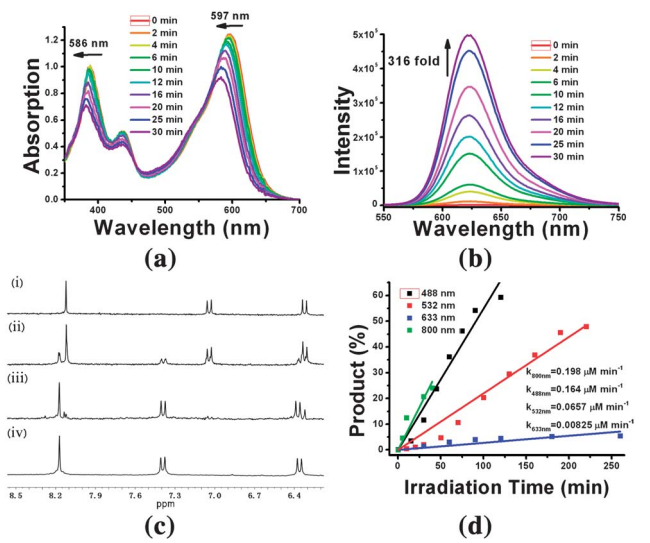

Fig. 1 Spectroscopic changes of (a) UV-vis absorption and (b) emission of **J-1**, upon irradiation with a 532 nm laser (20 mW). (c) Changes of ^{1}H NMR signals of **J-1** in the aromatic region, on exposure to sunlight for (i) 0 h, (ii) 2 h, (iii) 4 h, and (iv) **J-2**. (d) Time courses of photoactivation of **J-1** at 488 (5 mW), 532 (5 mW), 633 (5 mW), 800 nm (average power 300 mW). The yields (%) of **J-2** were determined by comparison with the fluorescence intensity of synthetic **J-2**.

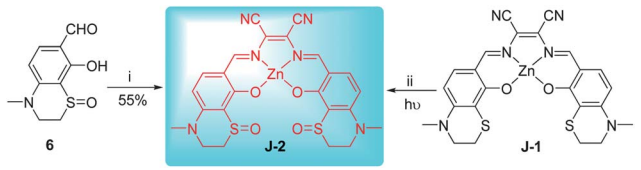

Scheme 2 Synthetic route for **J-2**: (i) $Zn(OAc)_2 \cdot 2H_2O$, 2,3-diaminomaleonitrile, EtOH; (ii) light irradiation.

Table 1 Photophysical properties of **J-1** and **J-2**

Compound[a]	λ_{max}/nm (ε)[b]	λ_{em}/nm	Φ_F[c]
J-1	388 (2.93)/437 (1.46)/597 (3.61)	627	0.0033
J-2	381 (2.24)/436 (1.24)/586 (3.31)	623	0.81

[a] Compounds were dissolved in DMSO (20 μM). [b] ε: extinction coefficients, 10^4 M^{-1} cm^{-1}. [c] Quantum yields were measured using Rhodamine B in ethanol as reference.

measured by comparison of the fluorescence intensity of synthetic **J-2** (Fig. S4†). As shown in Fig. 1d, the laser at 488 nm displayed a much higher efficiency than those obtained at 532 and 633 nm, in terms of reaction rate (0.198 μM min^{-1}) and the yield (60%) in the initial 2 h. It is worth noting that, in the absence of oxygen, light irradiation does not result in "switched on" fluorescence, indicating a photooxygenation mechanism for the conversion of **J-1** to **J-2** (Fig. S5†). Most importantly, two photon photoactivation of **J-1** was achieved by continuous irradiation with a laser at 800 nm (300 mW) and the activation curve is shown in Fig. 1d (green line). In the initial 40 min, the reaction rate of **J-2** is comparable to that at 488 nm, and the emission increases *ca.* 100 fold at 623 nm using two photon photoactivation (Fig. S6†). Along with increasing irradiation time, the emission of **J-2** began to decrease due to the intrinsic higher power 2PFM laser used.[38] These results demonstrated the potential application of **J-1** as a one and two photon activatable fluorophore in cell imaging.

To further evaluate the photophysical properties of **J-1** and **J-2**, we carried out time-dependent density functional theory calculations as implemented in the Gaussian 09 package (Fig. 2 and Table S1†).[39] The UV-vis absorptions of **J-1** and **J-2** were studied with TDDFT calculations and the frontier MOs involved in the vertical excitation of **J-1** and **J-2** are presented. For **J-1**, the $S_0 \rightarrow S_1$ transition is composed of HOMO-1 → LUMO, as shown in Table S1.† The calculated oscillator strength (f) for the $S_0 \rightarrow S_1$ transition is 0.0035, which is a forbidden transition ($f < 0.01$), suggesting that S_1 state of **J-1** is a dark state. The maximum transition probability occurs in the S_3 state with maximum oscillator strength ($f = 0.72$), and the major character is HOMO-2 → LUMO. The $S_0 \rightarrow S_2$ transition is also allowable ($f > 0.1$) with a smaller oscillator strength ($f = 0.27$), in which the major character is HOMO → LUMO (86%). Thus, for **J-1**, we focused on S_3 state with a dominant HOMO-2 → LUMO transition and an S_1 state with the contribution between LUMO and HOMO-1 in Fig. 2. For **J-2**, the TDDFT calculations were based on the optimized ground state (S_0) geometry, a low-lying transition-dipole-allowed S_0 to S_1 excitation (HOMO → LUMO), with an oscillator strength $f = 0.9721$. The HOMO and LUMO molecular orbitals (MO) are localized on the phenyl-CN unit. Thus, based on the experimental and theoretical calculations, the lack of emission of **J-1** can be attributed to the dark state S_1, induced by the thioether moiety which serves as an electron donor; after photosulfoxidation, $S_0 \rightarrow S_1$ is an allowed transition due to lowering of the energy of HOMO-1 and S_1 state will probably be emissive. This fluorescence OFF–ON switching effect is in line with the experimental results.

To demonstrate the applications of **J-1** in cell imaging, the cell viabilities of **J-1** and **J-2** were assessed first. MTT results revealed that both **J-1** and **J-2** have very low cytotoxicities in L6 myoblasts over a period of 24 h at concentrations of 2, 5, 8 and 10 μM (Fig. S7†). The phototoxicity of **J-1** is also very low even when the concentration is as high as 10 μM (Fig. S8†). Intracellular photoactivation of **J-1** was performed on L6 myoblasts by laser scanning confocal microscopy with a 543 nm laser. Upon irradiation, a maximum increase (6 fold) of the fluorescence intensity was detected within 2 min (Fig. 3). From the time course plot of fluorescence intensity *vs* irradiation time, fluorescence became constant after 2 mins (Fig. 3b). From Fig. 3c, the intracellular emission spectrum of photoactivated **J-1** was identical to that of **J-2**, indicating that photosulfoxidation occurs in living cells.

The subcellular localizations of **J-1** and **J-2** were examined by colocalization analysis with organelle markers such as LysoTracker Green DND-26, Hoechst 33582, MitoTracker Green and calcein-AM. Through the analysis of Pearson's coefficients with the ImageJ program, we found that the activated **J-1** was distributed in the cytoplasmic matrix (Pearson's coefficient: 0.78, Fig. S9†) whereas **J-2** was localized in lysosomes (Pearson's coefficient: 0.73, Fig. S10†). Interestingly, along with increasing incubation time, the photoactivated **J-1** tends to accumulate in lysosomes where **J-2** was mainly located.

To excluding the possibility of cellular ROS effect, a spatially controlled experiment was carried out by exposing a select population of cells to a 543 nm laser. After 2 min, enhanced fluorescence (5 times) was observed only in cells in the irradiation region and the rest remained fluorescence silent (Fig. S11†). These results strongly suggest that light irradiation is the main factor for "switching on" the fluorescence of **J-1** intracellularly.

Two photon activation of **J-1** was performed in living L6 myoblasts using a pulsed 840 nm laser. As shown in Fig. 4, **J-1** was activated with a roughly 2500-fold maximum fluorescence intensity increase after 10 min. Comparing the two time course plots (Fig. 3b and 4b), two photon activation of **J-1** was slower than one photon activation, but exhibits a much higher signal-to-noise contrast (ca. 2500-fold), due to the practically zero background. This is the advantage of two photon activatable fluorophores and would be important to achieve high temporal and spatial resolution in cell imaging.

Since the fluorescence of **J-1** can be "switched on" in live cells by one and two photon irradiation, we further investigated its application in *C. elegans*, which is a living model organism for *in vivo* studies. *C. elegans* were grown on nematode growth media (NGM) agar plates with a mixture of B-growth medium and 5 μM **J-1** at 20 °C for 24 h. For imaging, the worms were transferred onto an agar cushion on a glass slide, anesthetized, and then sealed with a glass cover slip.

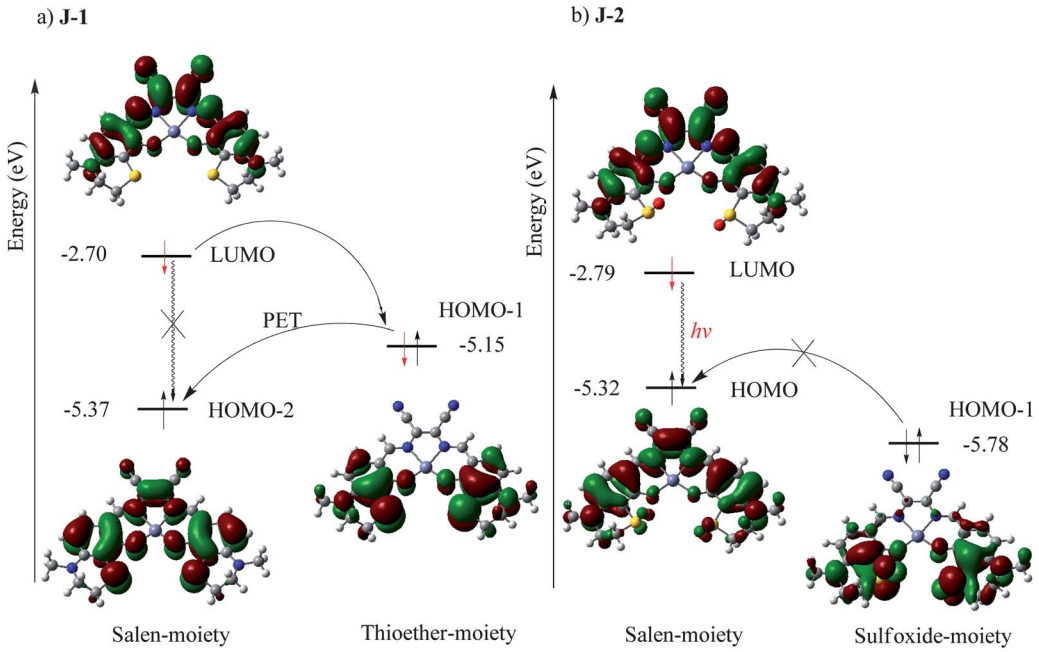

Fig. 2 Frontier molecular orbital energy illustrations show the relative energetic dispositions of the orbitals of the two moieties in **J-1** and **J-2**: (a) the fluorescence is quenched by intramolecular PET from the electron donating thioether moiety to the first excited single state of the ZnSalen; (b) photosulfoxidation of the thioether moiety lowers the energy of the HOMO-1 and prevents PET and fluorescence of ZnSalen is "switched on".

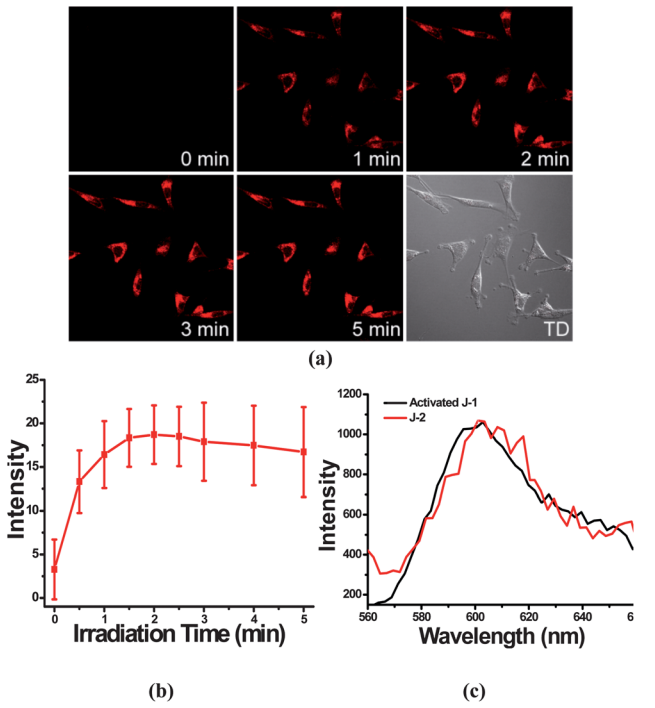

Fig. 3 Time course of photoactivation of **J-1** in L6 myoblasts. (a) Confocal images of cells loaded with 2 μM **J-1** during activation with 543 nm laser light. (b) Plot of the fluorescence intensity changes (mean ± SD, *ca.* 30 cells). (c) Emission spectra of activated **J-1** and **J-2** in cells.

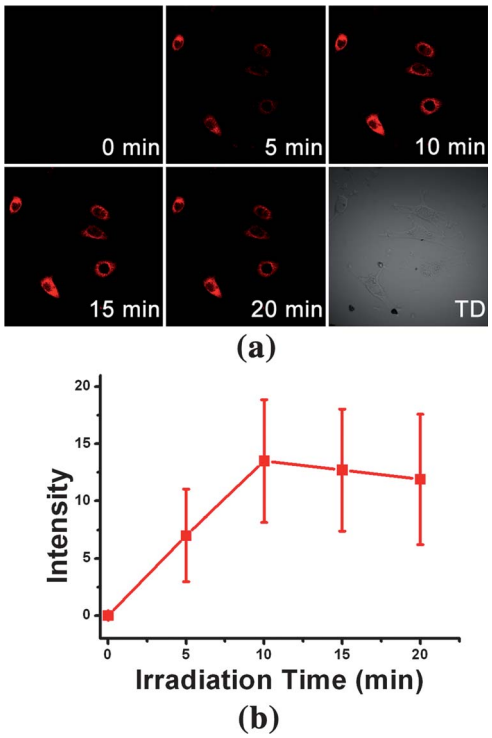

Fig. 4 (a) Time-lapsed two photon confocal micrographs of **J-1** treated L6 myoblasts, activated with a pulsed 840 nm laser. Cells were treated with 5 μM of **J-1** for 24 h in the dark. (b) Plot of the fluorescence intensity changes (mean ± SD, *ca.* 30 cells).

As shown in Fig. 5, after irradiation by 543 nm or pulsed 840 nm laser, a fluorescence intensity increase (*ca.* 5 times) of **J-1** treated *C. elegans* were observed in both one and two photon images. These results indicate that **J-1** can be taken up by *C. elegans* as well as activated by one and two photon lasers efficiently *in vivo*.

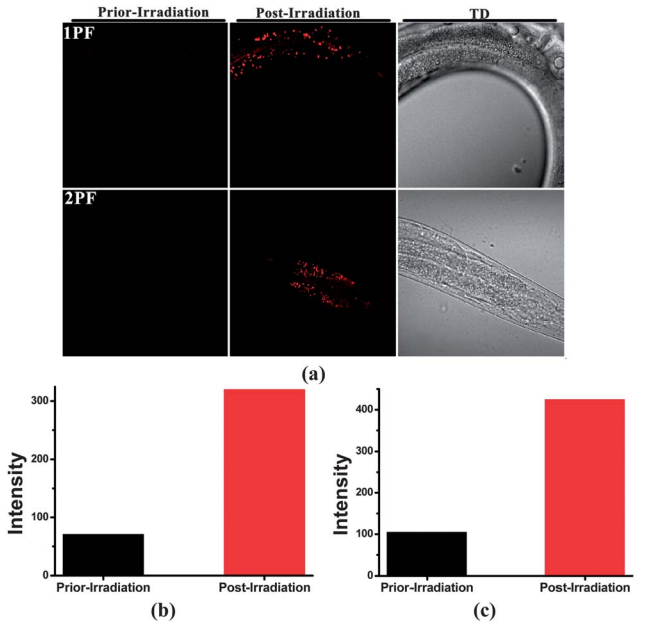

Fig. 5 One and two photon activation of **J-1** in *C. elegans* (N2 strain). (a) One and two photon fluorescence images of **J-1** prior to irradiation and after irradiation (one photon irradiation: 543 nm laser for 10 min, two photon irradiation: pulsed 840 nm laser for 15 min). (b) Plot of the fluorescence intensity change for one photon activation. (c) Plot of the fluorescence intensity change for two photon activation.

Conclusion

We have described the design of one and two photon activatable ZnSalen by photosulfoxidation beyond the "photouncaging" strategy. Upon light irradiation, **J-1** exhibited a high activation efficiency and obtained 316- and 100-fold fluorescence increases by one and two photon excitation, respectively. We also demonstrated the application of **J-1** in living cells by one and two photon fluorescence microscopies. A high signal-to-noise contrast (2500-fold) was achieved by irradiation with an 840 nm laser using two photon fluorescence microscopy. More importantly, its photoactivation nature was also implemented in a model living organism. Combined with other attractive features in a biological context, such as good membrane permeability and low cytotoxicity, further design and application of ZnSalens as a novel type of photoactivatable fluorophore is promising for super resolution microscopies such as PALM, STED and STORM.

Acknowledgements

This project was supported by the National Scientific Foundation of China (grant no. 20971007) and National Key Basic Research Support Foundation of China (NKBRSFC) (2010CB912302). Y. H. thanks the National Funding for Fostering Talents of Basic Sciences (J0630421).

Notes and references

1 M. Irie, *Chem. Rev.*, 2000, **100**, 1683–1684.
2 M. Tomasulo, E. Deniz, R. J. Alvarado and F. M. Raymo, *J. Phys. Chem. C*, 2008, **112**, 8038–8045.
3 I. Yildiz, E. Deniz and F. M. Raymo, *Chem. Soc. Rev.*, 2009, **38**, 1859–1867.
4 T. Fukaminato, *J. Photochem. Photobiol., C*, 2011, **12**, 177–208.
5 L. M. Wysocki and L. D. Lavis, *Curr. Opin. Chem. Biol.*, 2011, **15**, 752–759.
6 W.-H. Li and G. Zheng, *Photochem. Photobiol. Sci.*, 2012, **11**, 460–471.
7 G. Lukinavičius and K. Johnsson, *Curr. Opin. Chem. Biol.*, 2011, **15**, 768–774.
8 E. Betzig, G. H. Patterson, R. Sougrat, O. W. Lindwasser, S. Olenych, J. S. Bonifacino, M. W. Davidson, J. Lippincott-Schwartz and H. F. Hess, *Science*, 2006, **313**, 1642–1645.
9 M. J. Rust, M. Bates and X. Zhuang, *Nat. Methods*, 2006, **3**, 793–796.
10 M. Fernandez-Suarez and A. Y. Ting, *Nat. Rev. Mol. Cell Biol.*, 2008, **9**, 929–943.
11 R. Henriques, C. Griffiths, E. Hesper Rego and M. M. Mhlanga, *Biopolymers*, 2011, **95**, 322–331.
12 R. E. Thompson, D. R. Larson and W. W. Webb, *Biophys. J.*, 2002, **82**, 2775–2783.
13 M. Fernandez-Suarez and A. Y. Ting, *Nat. Rev. Mol. Cell Biol.*, 2008, **9**, 929–943.
14 S. W. Hell, *Science*, 2007, **316**, 1153–1158.
15 S. J. Lord, N. R. Conley, H.-l. D. Lee, R. Samuel, N. Liu, R. J. Twieg and W. E. Moerner, *J. Am. Chem. Soc.*, 2008, **130**, 9204–9205.
16 V. N. Belov, C. A. Wurm, V. P. Boyarskiy, S. Jakobs and S. W. Hell, *Angew. Chem., Int. Ed.*, 2010, **49**, 3520–3523.
17 A. P. Pelliccioli and J. Wirz, *Photochem. Photobiol. Sci.*, 2002, **1**, 441–458.
18 Z. Yu, L. Y. Ho and Q. Lin, *J. Am. Chem. Soc.*, 2011, **133**, 11912–11915.
19 D. Puliti, D. Warther, C. Orange, A. Specht and M. Goeldner, *Bioorg. Med. Chem.*, 2011, **19**, 1023–1029.
20 L. Donato, A. Mourot, C. M. Davenport, C. Herbivo, D. Warther, J. Léonard, F. Bolze, J.-F. Nicoud, R. H. Kramer, M. Goeldner and A. Specht, *Angew. Chem., Int. Ed.*, 2012, **51**, 1840–1843.
21 P. Neveu, I. Aujard, C. Benbrahim, T. Le Saux, J.-F. Allemand, S. Vriz, D. Bensimon and L. Jullien, *Angew. Chem., Int. Ed.*, 2008, **47**, 3744–3746.
22 K. Dakin and W.-H. Li, *Nat. Methods*, 2006, **3**, 959.
23 Q. Zhao, C. Huang and F. Li, *Chem. Soc. Rev.*, 2011, **40**, 2508–2524.
24 K. K.-W. Lo, A. W.-T. Choi and W. H.-T. Law, *Dalton Trans.*, 2012, **41**, 6021–6047.
25 C. Li, M. Yu, Y. Sun, Y. Wu, C. Huang and F. Li, *J. Am. Chem. Soc.*, 2011, **133**, 11231–11239.
26 M.-W. Louie, T. T.-H. Fong and K. K.-W. Lo, *Inorg. Chem.*, 2011, **50**, 9465–9471.
27 P. Wu, E. L.-M. Wong, D.-L. Ma, G. S.-M. Tong, K.-M. Ng and C.-M. Che, *Chem.–Eur. J.*, 2009, **15**, 3652–3656.
28 W. Tan, J. Zhou, F. Li, T. Yi and H. Tian, *Chem.–Asian J.*, 2011, **6**, 1263–1268.
29 Y. Hai, J.-J. Chen, P. Zhao, H. Lv, Y. Yu, P. Xu and J.-L. Zhang, *Chem. Commun.*, 2011, **47**, 2435–2437.
30 Y.-B. Cai, J. Zhan, Y. Hai and J.-L. Zhang, *Chem.–Eur. J.*, 2012, **18**, 4242–4249.
31 C.-C. Kwok, S.-C. Yu, I. H. T. Sham and C.-M. Che, *Chem. Commun.*, 2004, 2758–2759.
32 P. Wang, Z. Hong, Z. Xie, S. Tong, O. Wong, C.-S. Lee, N. Wong, L. Hung and S. Lee, *Chem. Commun.*, 2003, 1664–1665.
33 X. Wang, X. Tian, Q. Zhang, P. Sun, J. Wu, H. Zhou, B. Jin, J. Yang, S. Zhang, C. Wang, X. Tao, M. Jiang and Y. Tian, *Chem. Mater.*, 2012, **24**, 954–961.
34 X. Zhang, L. Chi, S. Ji, Y. Wu, P. Song, K. Han, H. Guo, T. D. James and J. Zhao, *J. Am. Chem. Soc.*, 2009, **131**, 17452–17463.
35 A. P. de Silva, H. Q. N. Gunaratne, T. Gunnlaugsson, A. J. M. Huxley, C. P. McCoy, J. T. Rademacher and T. E. Rice, *Chem. Rev.*, 1997, **97**, 1515–1566.
36 S. M. Bonesi, I. Manet, M. Freccero, M. Fagnoni and A. Albini, *Chem.–Eur. J.*, 2006, **12**, 4844–4857.
37 E. Baciocchi, T. D. Giacco, F. Elisei, M. F. Gerini, M. Guerra, A. Lapi and P. Liberali, *J. Am. Chem. Soc.*, 2003, **125**, 16444–16454.
38 K. Svoboda and R. Yasuda, *Neuron*, 2006, **50**, 823–839.
39 M. J. Frisch, G. W. Trucks, H. B. Schlegel, G. E. Scuseria, M. A. Robb, J. R. Cheeseman, G. Scalmani, V. Barone, B. Mennucci, G. A. Petersson, H. Nakatsuji, M. Caricato, X. Li, H. P. Hratchian, A. F. Izmaylov, J. Bloino, G. Zheng,

J. L. Sonnenberg, M. Hada, M. Ehara, K. Toyota, R. Fukuda, J. Hasegawa, M. Ishida, T. Nakajima, Y. Honda, O. Kitao, H. Nakai, T. Vreven, J. A. Montgomery, Jr., J. E. Peralta, F. Ogliaro, M. Bearpark, J. J. Heyd, E. Brothers, K. N. Kudin, V. N. Staroverov, R. Kobayashi, J. Normand, K. Raghavachari, A. Rendell, J. C. Burant, S. S. Iyengar, J. Tomasi, M. Cossi, N. Rega, J. M. Millam, M. Klene, J. E. Knox, J. B. Cross, V. Bakken, C. Adamo, J. Jaramillo, R. Gomperts, R. E. Stratmann, O. Yazyev, A. J. Austin, R. Cammi, C. Pomelli, J. Ochterski, R. L. Martin, K. Morokuma, V. G. Zakrzewski, G. A. Voth, P. Salvador, J. J. Dannenberg, S. Dapprich, A. D. Daniels, O. Farkas, J. B. Foresman, J. V. Ortiz, J. Cioslowski and D. J. Fox, *GAUSSIAN 09 (Revision A.2)*, Gaussian, Inc., Wallingford, CT, 2009.

